Spatial Analysis of Urban Growth Impacts on Vegetative Greenness with Landsat TM Data

Qihao Weng
Department of Geography, Geology, and Anthropology
Indiana State University
Terre Haute, IN 47809, USA
E-mail: geweng@scifac.indstate.edu

C. P. Lo
Department of Geography
University of Georgia
Athens, Georgia 30602, USA
E-mail: chpanglo@uga.edu

Abstract

Landsat Thematic Mapper (TM) data have been used to monitor land cover types and to estimate biophysical parameters. However, studies examining the spatial relationships between land cover change and biophysical parameters are generally lacking. With the integration of remote sensing and Geographic Information Systems (GIS), these relationships can be better explored. The research reported in this paper applies this integrated approach for detecting urban growth and assessing its impact on vegetative greenness in the Zhujiang Delta, China. Multi-temporal Landsat TM data were utilized to map urban growth and to extract and identify changes in vegetative greenness. GIS analyses were conducted to examine the changing spatial patterns of urban growth and greenness change. Statistical analyses were then used to examine the impact of urban growth on vegetative greenness. The results revealed that there was a notably uneven urban growth pattern in the delta, and urban development had reduced the scaled Normalized Difference Vegetation Index (NDVI) value by 30% in the urbanized area.

Introduction

Remote sensing has been used to monitor discrete land cover types by spectral classification and to estimate biophysical characteristics of land surfaces via linear relationships with spectral reflectances or indices (Steininger, 1996). Landsat TM and other remote sensing data have been found effective in detecting urban land use and land cover change (Ehlers *et al.*, 1990; Treitz *et al.*, 1992; Harris and Ventura, 1995). Post-classification comparison and multi-date composite image change detection are the two most commonly used methods in change detection. The first method classifies each image and then compares the two maps on a pixel-by-pixel basis using a change detection matrix. This method can provide "from-to" information for each class, but the result of the comparison is subject to the accuracy of individual classifications (Jensen, 1996). The second method places rectified multi-date images in a single dataset, and analyzes the composite imagery in different ways such as unsupervised classification, principal component analysis, image differencing, and ratioing. The advantage of this method is that only a single classification is required. However, it suffers in labeling change classes, since little "from-to" change class information is available (Jensen, 1996).

Landsat TM imagery has been found useful in the following three areas of vegetation studies: (1) identifying and mapping vegetation types by spectral classification (Lo and Watson, 1994; Dymond *et al.*, 1996; Foody and Hill, 1996; Knick *et al.*, 1997); (2) monitoring succession and change (Jakubauskas and Price, 1994; Li *et al.*, 1994; Sader, 1994; Ekstrand, 1996); and (3) estimating biochemical and biophysical characteristics (Thenkabail *et al.*, 1994; Steininger, 1996). The Normalized Difference Vegetation Index (NDVI) has been widely applied for various purposes, including estimation of biomass and leaf area index (Lo and Watson, 1994), tropical secondary forest re-growth estimation (Steininger, 1996), and determining crop growth parameters (Thenkabail *et al.*, 1994). Most vegetation mapping has focused on forest (especially tropical forest) and agricultural areas.

Key Words: Remote sensing/GIS integration; Landsat TM data; Urban growth; Environmental impact.

Geocarto International, Vol. 16, No. 4, December 2001
Published by Geocarto International Centre, G.P.O. Box 4122, Hong Kong.

Few studies have examined the spatial relationships between urban land cover changes and biophysical parameters (Weng, 2001), in spite of the fact that the techniques for such studies have become mature in recent years because of advances in the technology of GIS and its integration with remote sensing. Traditionally, remote sensing and GIS have worked separately, making use of "spectral" and "spatial" techniques, respectively (Atkinson and Tate, 1999). The integration of the two technologies has led to an increased cross-fertilization of research ideas (Star, 1991; ASPRS, 1994; Hinton, 1996; Mesev, 1997; Star *et al.*, 1997). Recent research in remote sensing and GIS analysis have increasingly focused on modeling (e.g., characterization of spatial process or form) and validation, rather than solely the estimation of continuous (e.g., biomass, leaf area index) and categorical variables (i.e., classification) (Atkinson and Tate, 1999). Several recent studies have examined post-detection urban growth patterns and processes (Yeh and Li, 1996; 1997; 1999; Weng, 2001), while in vegetation studies, researchers attempt to analyze the spatial characteristics of biomass change (Sader *et al.*, 1990; Sader, 1994). However, few studies have attempted to link urban growth patterns and processes to the spatial characteristics of biomass change. This missing linkage has hindered modeling and assessing the dynamics of land use and land cover change, and impeded progress towards understanding of earth-atmosphere interactions, biodiversity loss, and global environmental change.

This paper presents a method that combines remote sensing, GIS, and spatial analysis to examine the impacts of urban growth on vegetative greenness, which refers to the total amount of aboveground green plants within the instantaneous field of view (IFOV) of the Landsat TM sensor. Using 1989 and 1997 Landsat TM imagery of the Zhujiang Delta of South China, the specific objectives of this paper are: (1) to analyze urban land cover changes during the 8-year study period and their spatial patterns; (2) to evaluate vegetative greenness changes and their spatial patterns; and (3) to examine the spatial relationships between the urban growth and vegetative greenness changes.

Methods

Study area

The Zhujiang (literally "the Pearl River") Delta, located between latitudes 21°40'N and 23°00'N, and longitudes 112°00'E and 113°20'E, is the third largest river delta in China. This study focuses on the core area of the delta, which has an area of 15,112 sq. km (Figure 1). Geomorphologically, the delta consists of three sub-deltas formed by sediments, namely, the Xijiang, Beijiang, and Dongjiang Deltas. The process of sedimentation still continues today, and the delta is extending seaward at a rate of 40 meters per year (Gong and Chen, 1964). The climate of the delta is basically tropical with an average annual temperature between 21°C and 23°C, and an average precipitation from 1,600 to 2,600 mm. Natural vegetation is predominantly of evergreen types.

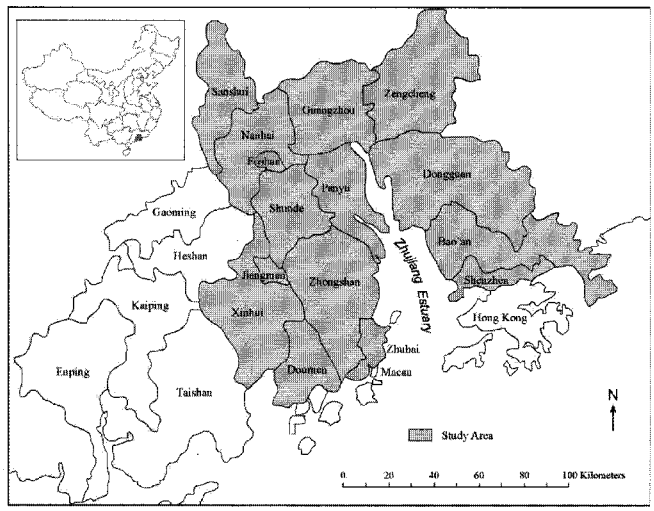

Figure 1 A map of the study area.

Economically, the Zhujiang Delta is the largest area of economic concentration in South China. Since 1978, the delta has had a dramatic economic expansion under China's economic reform policies, and therefore has been regarded as a model for Chinese regional development. The establishment of Special Economic Zones and the Economic Open Zone has stimulated foreign firms to locate their factories there as village-township enterprises. The labor-intensive industries, in association with the cash crop production, have transformed the spatial economy of the delta (Lo, 1989; Weng, 1998).

The rapid economic development has brought about fundamental changes in land use and land cover patterns. Urban growth has accelerated, while agricultural lands are disappearing. Because of the lack of appropriate land use planning and the measures for sustainable development, rampant urban growth has been creating severe environmental consequences. Evaluating the pattern and process of urban growth and its environmental impacts have become important topics of concern.

Land cover classification and analysis

Land use and land cover patterns for 1989 and 1997 were mapped using Landsat TM data (Dates: December 13, 1989 and August 29, 1997). A modified version of the Anderson scheme of land use/cover classification was adopted (Anderson *et al.*, 1976). The categories include: (1) urban or built-up land, (2) barren land, (3) cropland (rice), (4) horticulture farms (primarily fruit trees), (5) dike-pond land, (6) forest, and (7) water.

Each Landsat image was rectified to a common UTM coordinate system based on 1:50,000 scale topographic maps. These data were resampled using the nearest neighbor algorithm, so that the original brightness values of pixels were kept unchanged. The resultant root mean squared error was found to be 0.73 pixel (or 21.9 m on the ground) for the 1989 scene, and 0.58 pixel (or 17.4 m on the ground) for the 1997 scene.

Since this study requires the detection of fine changes in surface reflectances for vegetative greenness analysis, radiometric correction became necessary. However, no ancillary data on the atmospheric conditions during the satellite overpasses were available to account for atmospheric differences between the two dates. A relative radiometric correction method using image regression (Jensen *et al.*, 1995; Jensen, 1996) was therefore employed, by which the brightness value of each pixel of the subject scene (the 1989 scene) was related to that of the reference image (the 1997 scene) band by band to produce a linear regression equation. This image normalization method can minimize or eliminate the effects caused by using historical remotely sensed images of nonaniversary dates with varying sun angle, atmospheric, and soil moisture conditions (Jensen, 1996, pp.116-119).

A supervised signature extraction with the maximum likelihood algorithm was employed to classify the Landsat images. Both statistical and graphical analyses of feature selection were conducted, and bands 2 (green), 3 (red), and 4 (near infrared) were found to be most effective in discriminating each class and thus, were used for classification. The feature selection process reduced the number of bands to be processed in the database. The accuracy of the classified maps was checked with a stratified random sampling method, by which 50 samples were selected for each land use and land cover category. The reference data was collected from field survey or from existing land use and cover maps that have been field-checked. Large-scale aerial photos were also employed as reference data in accuracy assessment when necessary.

In performing land use/cover change detection, a cross-tabulation detection method was adopted. Quantitative areal data of the overall land use/cover changes as well as gains and losses in each category between 1989 and 1997 were compiled. In order to analyze the nature, rate, and location of urban land change, urban and built-up lands were extracted from each original land-cover image. The two extracted images were then overlaid and recoded to obtain an urban land cover change (expansion) image.

This urban expansion image was combined with several geographic data sets to help analyze the patterns and processes of urban expansion. These layers include county/city boundaries, major roads, and major urban centers, and were downloaded from CIESIN's (Consortium for International Earth Science Information Network) GIS Data for China Times Series Administrative Regions, which were prepared by CIESIN, Chinese Academy of Surveying and Mapping, and the University of Washington. The needed data were extracted in a vector GIS environment and then converted into raster format with a grid resolution of 30 meters. The county/city boundary image was utilized to find urban land change information within each county/city.

Because proximity to a certain feature (such as major roads or urban centers) has an important implication in urban land development, urban expansion processes often show an intimate relationship with distance from these geographic features. Using a GIS buffer function, two buffer images were generated. The first buffer image shows ten buffer zones around major roads, each with a width of 500 meters (0-500m, 500-1000m, 1000-1500m, and so on). The second buffer image was created to delineate ten buffer zones around the urban centers, each having a width of 1000 meters (0-1000m, 1000-2000m, 2000-3000m, and so on). The buffer images were overlaid with the urban expansion image to calculate the amount of urban expansion in each zone. The density of urban expansion was then calculated by dividing the amount of urban expansion by the land area in each buffer zone. These values of density were used to construct a distance decay function of urban expansion.

The density values in the concentric zones of an urban center were further used for computing the entropy index for each city to reveal the degree of urban dispersion. The index is one version of the Theil Index of inequality, derived from the notion of entropy in information theory (Theil, 1967). The idea behind information entropy is that unlikely events receive more weight than those that conform to expectations (Nissan and Carter, 1994). This measure is expressed as

$$H(y) = \sum_{i=1}^{N} y_i \log(1/y_i) \qquad (1)$$

where y_i is the share of a geographic variable in the ith region in a total of N regions, and it is required to be non-negative and to sum to 1:

$$\sum_{i=1}^{N} y_i = 1 \qquad y_i >= 0 \quad i = 1,...,N \qquad (2)$$

The entropy index always has a value between 0 and 1. If one share is 1 and all others are 0, then H(y) = 0 (the minimum entropy value) will be the maximum degree of concentration. If all shares are equal and hence equal to 1/N, then H(y) = log N, which is the maximum entropy value and also the minimum degree of concentration. Obviously, the larger the entropy index, the higher the degree of dispersion.

Vegetative greenness change analysis

To quantify and spatially analyze the vegetative greenness change, a change detection procedure was implemented. NDVI was computed for 1989 and 1997 from visible (0.63-0.69 (m) and near-infrared (0.76-0.90 (m) data to determine the amount of vegetative greenness. Although these two bands were radiometrically normalized to account for differences in atmospheric conditions, the values of NDVI may be scaled when comparing images from two different days or seasons. This is because the absolute values of NDVI tend to vary temporally in a non-systematic manner (Price, 1987; Che and Price, 1992). A scaled value of NDVI (N*) was computed according to the following formula (Gillies *et al.*, 1997):

$$N^* = \frac{NDVI - NDVI_O}{NDVI_S - NDVI_O} \qquad (3)$$

where $NDVI_O$ is the minimum value and $NDVI_S$ the maximum

value of NDVI in an image. Usually, NDVIo is associated with "water" while NDVIs is associated with "forest."

Image differencing was performed between the 1997 and 1989 N* images. This differencing image was thresholded into three gray levels to represent greenness increase, no change, and greenness decrease. The thresholds were determined interactively by overlaying and comparing the N* values with 1989 and 1997 false color composites. Next, two binary images were prepared of greenness increase and decrease by reclassifying the threshold image. Finally, each binary image was overlaid with each of the buffer images to compute the amount of greenness change within each zone.

Results and Analyses

Spatial patterns of urban growth

The overall accuracy of the land use/cover maps for 1989 and 1997 was determined to be 90.57 percent and 85.43 percent respectively (Tables 1 and 2). The KAPPA indices for the 1989 and 1997 maps were 0.89 and 0.83 respectively. Clearly, these data met the minimum standard of 85 percent stipulated by the USGS classification scheme (Anderson *et al.*, 1976). Overall, the user's and producer's accuracies were high. The accuracy is therefore sufficient for urban growth detection.

Table 3 shows the land use and land cover change matrix of the Zhujiang Delta from 1989 to 1997. From this table, it is clear that there has been a considerable change (12.82% of the total area) in land use and land cover in the study area during the 8-year period. Urban or built-up land and horticulture farms have increased in area (by 47.68% and 88.66% respectively), and cropland has decreased in area (by 48.37%).

The overlay of the 1989 and 1997 land use/cover map further indicates that of the 47.68% (65 690 hectares) increase in urban or built-up land, most results from cropland (37.92%) and horticulture farms (16.05%). Figure 2 shows the areal extent and spatial occurrence of the urban expansion. The overlay of this map with a city/county mask reveals the spatial occurrence of urban expansion within administrative regions. Table 4 shows that in absolute terms, the greatest urban expansion occurred in Dongguan (23479 hectares), Baoan (14941 hectares), Nanhai (8004 hectares), and Zhuhai (5869 hectares). However, in percentage term, the largest increase in urban or built-up land occurred in Zhuhai (1100%), followed by Shenzhen (307%), Baoan (233%), and Dongguan (126%). Massive urban sprawl in these areas can be ascribable to rural urbanization, which is a common phenomenon in post-reform China (Yeh and Li, 1999). Rapid urban

Table 1 Error matrix of the land use and land cover map, 1989.

	Reference Data											
Classified Data	UC	UB	BL	CR	HF	DP	FO	WA	**RT**	**CT**	**PA**	**UA**
UC	0	0	0	0	0	0	0	0	7	0		
UB	0	48	0	0	2	0	0	0	48	50	100 %	96.0 %
BL	6	0	44	0	0	0	0	0	44	50	100 %	88.0 %
CR	1	0	0	42	4	1	2	0	45	50	93.3 %	84.0 %
HF	0	0	0	1	45	0	4	0	54	50	83.3 %	90.0 %
DP	0	0	0	2	1	42	0	5	43	50	97.7 %	84.0 %
FO	0	0	0	0	2	0	47	1	54	50	87.0 %	94.0 %
WA	0	0	0	0	0	0	1	49	55	50	89.1 %	98.0 %
Column Total	7	48	44	45	54	43	54	55				
Overall Accuracy	90.57%											
KAPPA index	0.89											
Total number of samples	350											

Note: UC-Unclassified; UB-Urban or Built-up Land; BL-Barren Land; CR-Crop Land; HF-Horticulture Farm; DP-Dike-pond Land; FO-Forest; WA-Water.
RT-Reference Total; CT-Classified Total; PA-Producer's Accuracy; UA-User's Accuracy.

Table 2 Error matrix of the land use and land cover map, 1997.

	Reference Data											
Classified Data	UC	UB	BL	CR	HF	DP	FO	WA	**RT**	**CT**	**PA**	**UA**
UC	0	0	0	0	0	0	0	0	21	0		
UB	1	42	2	0	5	0	0	0	42	50	100 %	84.0 %
BL	20	0	30	0	0	0	0	0	32	50	93.8 %	60.0 %
CR	0	0	0	38	11	0	1	0	40	50	95.0 %	76.0 %
HF	0	0	0	2	47	1	0	0	65	50	72.3 %	94.0 %
DP	0	0	0	0	2	43	0	5	44	50	97.7 %	86.0 %
FO	0	0	0	0	0	0	49	1	50	50	98.0 %	98.0 %
WA	0	0	0	0	0	0	0	50	56	50	89.3 %	100 %
Column Total	21	42	32	40	65	44	50	56				
Overall Accuracy	85.43%											
KAPPA index	0.83											
Total number of samples	350											

Note: UC-Unclassified; UB-Urban or Built-up Land; BL-Barren Land; CR-Crop Land; HF-Horticulture Farm; DP-Dike-pond Land; FO-Forest; WA-Water.
RT-Reference Total; CT-Classified Total; PA-Producer's Accuracy; UA-User's Accuracy.

development in the form of small towns in the east side of the delta is highly influenced by the investment from Hong Kong. In contrast, those old cities, such as Guangzhou and Foshan, do not show a rapid increase in urban or built-up land because they have no land to expand further (as they have already expanded fully in the past) and the concentration of urban enterprises in the city proper. Although Shenzhen and Zhuhai were designated as Special Economic Zones at the same time, the pace of urbanization in the two cities is quite different. Urban development in Shenzhen has mostly been completed in the 1980s, while Zhuhai's urban expansion appears primarily during the period of 1989-97 (5869 hectares).

The urban expansion processes were further examined by plotting a distance decay curve from a major road (Figure 3) and establishing a mathematical equation. The result indicates that the density of urban expansion decreases as the distance increases away from a major road. Most urban expansion (66 percent) can be observed within a distance of 2,000 meters from a major road. This rapid urban expansion pattern is vividly illustrated along the expressway from Guangzhou to Hong Kong as seen in Figure 3, where Hong Kong investors seek sites for constructing factories and housing. Using the technique of best-fit, the mathematical relationship between the density of urban expansion (Y) and the distance from a major road (X) can be established as follows:

$$Y=0.2237e^{-0.00046x} \qquad (4)$$

The average density of urban expansion in each buffer zone around the urban centers is plotted against the distance from an urban center (Figure 4). The results show that as the distance increases away from an urban center, the density of urban expansion increases first to a peak and then slowly decreases. The break line has an average distance of 3,500 meters from an urban center. A further inquiry of the density distribution curve reveals that the majority of urban expansion (72.85 percent) occurred in the zone between 2,500 and 5,500 meters. Using a best-fit technique, a mathematical relationship between the density (Y) and the distance (X) can also be established:

$$Y = \begin{cases} -0.0058+0.000089\ X\ (X \le 3500\ meters) \\ 18.98*e^{-0.00088}\ X\ (X>3500\ meters) \end{cases} \qquad (5)$$

The computation of the entropy index indicates that the cities in the delta have an average entropy of 0.64, implying a relatively high degree of urban dispersion. However, significant differences of the entropy index value persist among the cities examined. Two major types of urban expansion can be identified: concentrated and dispersed type. Guangzhou and Jiangmen belong to the first type, having an average entropy index of 0.42. Most of the urban expansion in these cities is far away from the city centers. Guangzhou's urban development primarily occurs 6,500 meters outside the city center, while Jiangmen's urban development occurs 5,500 meters away from its center. The second type of urban expansion pattern has an average entropy index of 0.69, including Zengcheng, Nanhai, Dongguan, Shunde, Xinhui, Zhongshan, Shenzhen, and Zhuhai. Urban development in these cities is found to be more scattered, and spreads over to the suburban and surrounding rural areas as seen from the satellite images. The urban expansion zone for these cities lies between 2,500 and 8,500 meters from city centers.

These differences in urban expansion patterns reflect, to a large extent, the difference in the history of urban development. Guangzhou and Jiangmen have long been designed to function as pure urban centers, supported primarily by secondary and tertiary production. The majority of the land near the urban centers was filled before China initiated the economic reform policy in 1978. Recent urban development in these cities has led to a search for spare land

Table 3 Land use/cover change matrix, 1989-97 (in hectares).

	1997								
1989	Unclassified	Urban or built-up land	Barren land	Cropland	Horticulture Farms	Dike-pond land	Forest	Water	**1989 Total**
Unclassified	3918240	0	0	0	0	0	0	0	3918240
Urban or Built-up	0	54189	493.38	20890.8	35816.8	15887.4	3082.77	7407.36	137768
Barren Land	0	11603.4	661.77	4156.02	8690.4	1285.47	1414.53	1293.75	29105.4
Cropland	0	77151.5	4651.11	152400	215536	55272.7	44497.1	29258.4	578767
Horticulture Farms	0	32660.8	3775.23	44972.9	132372	12850.2	43752.3	8222.22	278605
Dike-pond land	0	14902.8	321.03	33931.4	20238.6	42489.7	2640.96	31327.4	145852
Forest	0	8378.64	3028.59	26294.7	102589	3906.72	128048	5436.81	277683
Water	0	4571.37	472.95	16156.6	10366.1	11179.7	1845.09	64414.3	109006
1997 Total	3918240	203458	13404.1	298803	525609	142872	225281	147360	5475026.88
Change (ha)	0	65690	- 15701.3	- 279964	247004	- 2980	- 52402	38354	702095.3
Change (%)	0	+ 47.68	- 53.93	- 48.37	+ 88.66	- 0.02	- 18.87	+ 3.19	12.82

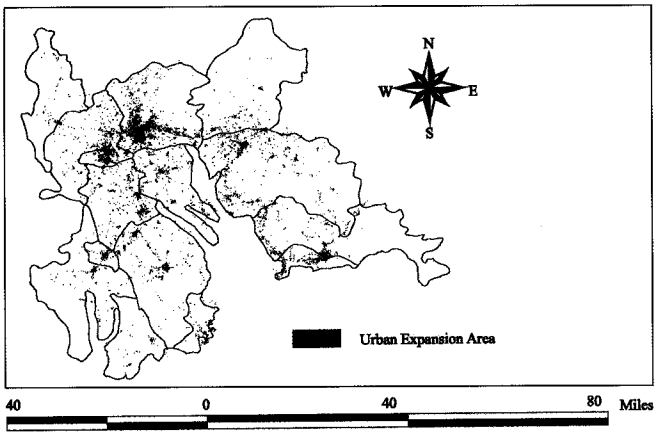

Figure 2 A map of urban expansion in the Zhujiang Delta, 1989-97

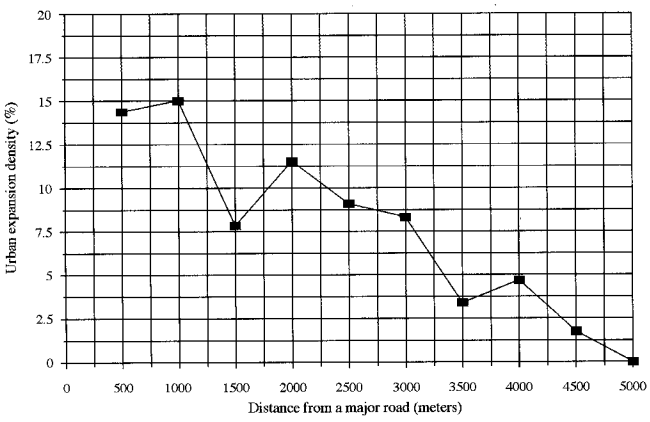

Figure 3 Urban expansion density as a function of the distance from a major road

in the suburban areas, which are far from the city center. In contrast, cities that exhibited a wide dispersal pattern were basically county-seat towns or even small towns before 1978. Urban development in these cities therefore has had much more freedom, and is subject to the influence of the economic reform policies. Three factors have contributed to this highly dispersed urban development pattern, including rural urbanization, the influence of Hong Kong and foreign investment, and the lack of proper urban planning.

Characteristics of vegetative greenness change

The average NDVI value by land cover type was computed for both 1989 and 1997 (Table 5). In 1989, the value of NDVI varied from -0.26 to +0.32, with a mean value of 0.03. In 1997, the value of NDVI ranged from -0.28 to +0.37, averaging at 0.032. Table 5 further reveals that each land cover type has a distinguishable signature of vegetative greenness. In both years, forests exhibit the highest NDVI value (0.1577 in 1989 and 0.1604 in 1997), followed by horticulture farms (0.0901 in 1989 and 0.0986 in 1997), and cropland (0.0097 in 1989 and 0.0098 in 1997). In contrast, water has the lowest value of NDVI in both 1989 (-0.0862) and 1997 (-0.0864), owing to its larger visible reflectance over near-infrared reflectance. A dike-pond land also

Table 4 Satellite-detected Urban Expansion in the Zhujiang Delta, 1989-97

City/County	Urban Area 1989 (ha)	Urban Area 1997 (ha)	Change (%)	Change
Baoan	6403	21344	14941	233
Dongguan	18676	42155	23479	126
Doumen	2134	3735	1601	75
Foshan	6403	6937	534	8
Guangzhou	23479	28281	4802	20
Jiangmen	1601	3735	2134	133
Nanhai	13340	21344	8004	60
Panyu	7471	8538	1067	14
Sanshui	2134	2134	0	0
Shenzhen	1050	4269	3219	307
Shunde	6403	10138	3735	58
Xinhui	5870	7471	1601	27
Zengcheng	5869	5869	0	0
Zhongshan	13340	16542	3202	24
Zhuhai	534	6403	5869	1100

Table 5 Average NDVI values by land cover types

Land Cover	1989	Standard Deviation (±)	1997	Standard Deviation (±)
Urban or Built-up Land	-0.0852	0.0385	-0.0853	0.0424
Barren Land	-0.0435	0.0371	-0.0405	0.0396
Cropland	0.0097	0.0646	0.0098	0.0685
Horticulture Farms	0.0901	0.0725	0.0986	0.0733
Dike-pond Land	-0.0545	0.0383	-0.0542	0.0377
Forest	0.1577	0.0640	0.1604	0.0499
Water	-0.0862	0.0829	-0.0864	0.0917

produced a low value of NDVI, since it normally consists of 60 percent water surface and 40 percent dike on which various types of crops were planted. The NDVI value of dike-pond land was -0.0545 in 1989 and -0.0542 in 1997. Urban/built-up land and barren land, which have similar reflectance in the two bands, produced NDVI values near zero.

The standard deviations of the NDVI for water were the highest in both years (0.0829 in 1989 and 0.0917 in 1997), indicating the heterogeneous nature of water body. This heterogeneity is largely caused by the differences in the amount of sediments in the water. Major variations exist among rivers, lakes, near-shore ocean, and offshore ocean. On the other hand, the standard deviations of NDVI for construction sites, urban or built-up land, and dike-pond land were small. These small values are the result of homogeneity of each land cover type.

The detection of vegetative greenness change requires comparing scaled NDVI (N*) values between two years by

land cover type. Table 6 shows the N* values in 1989 and 1997. A vegetative greenness change image (Figure 5) was produced according to the procedures described above. The overlay of this image with the urban expansion image gave rise to a change detection map of vegetative greenness. The computed statistics based on this map shows that the urban land development has caused a reduction of N* value of 0.10, with a standard deviation of 0.11. This implies that urban development has decreased the greenness and degraded the biophysical environment.

Spatial patterns of vegetative greenness change

From Figure 5, it is clear that vegetative greenness increase took place in most of the surrounding areas, particularly to the north of the Delta, where major landforms are mountains that average from 500 to 1,000 meters in height. The increase in vegetative greenness in these areas is probably related to the call of local governments for afforestation in barren hills, slash reforestation, and transformation of low-yield forests (Statistical Bureau of Guangdong, 1998). Inside the delta itself, vegetative greenness increase is concentrated in the western part, such as the counties of Xinhui, Doumen, Kaiping, and Gaoming. In addition, some areas in the northern part of Guangzhou and Zengcheng had also experienced a greenness increase during the period of 1989 to 1997. The spatial pattern of vegetative greenness increase was strongly affected by its topography. The majority of the increase was observed in dissected hills that range from 200 to 400 meters in height.

Vegetative greenness decrease appeared in all central parts of the delta. A total of 3.11 percent (313,546 hectares) of the area exhibited decreased biomass. The spatial pattern of greenness decrease was first explored in terms of road proximity. The density of greenness decrease in each buffer zone around the major roads was computed by dividing the total area of greenness decrease by the total area of the buffer zone. The result indicates that decreases in the density of vegetative greenness decline rapidly as the distance increases away from a major road. Forty-four percent of the greenness decrease was within 5 km of the major roads. Furthermore, a Pearson's correlation was computed between the density of greenness decrease and the density of urban expansion. A coefficient value of 0.63 was obtained at the significant level of 0.05, indicating that the mapped pattern of greenness decrease was closely related with that of urban expansion.

The spatial pattern of vegetative greenness change was further explored by relating the density

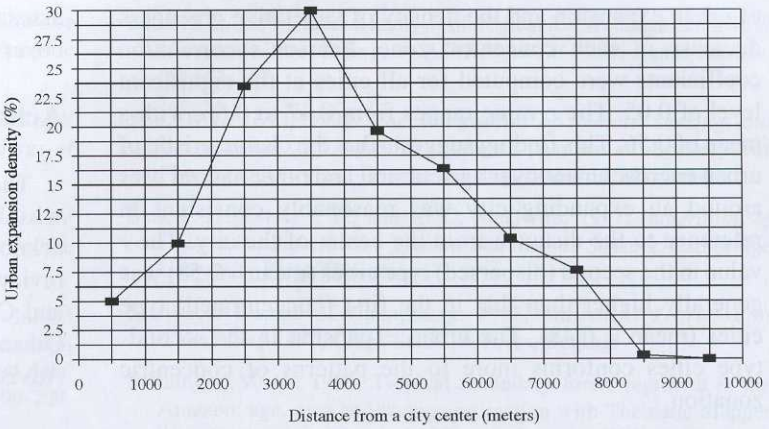

Figure 4 Urban expansion density as a function of the distance from an urban center

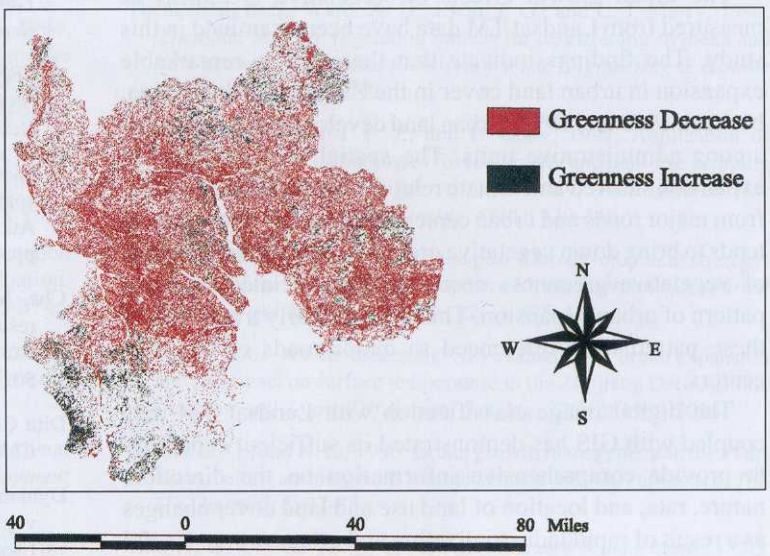

Figure 5 Biomass Change in the Zhujiang Delta, 1989-97.

Table 6 Scaled NDVI values by land cover types

Land Cover	1989	Standard Deviation (±)	1997	Standard Deviation (±)
Urban or Built-up Land	0.0041	0.5113	0.0045	0.5327
Barren Land	0.1751	0.5055	0.1860	0.5034
Cropland	0.3932	0.6183	0.3898	0.6427
Horticulture Farms	0.7228	0.6507	0.7496	0.6824
Dike-pond Land	0.1300	0.5105	0.1305	0.5355
Forest	1.000	0.6158	1.0000	0.6155
Water	0.0000	0.6933	0.0000	0.7346

of urban expansion and the density of vegetative greenness decrease in each concentric zone. Pearson's correlation coefficients were computed for all cities at the significant level of 0.05. The r value ranges from 0.47 to 0.66, with a mean of 0.56. This finding suggests that the characteristic of urban encroachment over agricultural and other natural uses around an expanding city was reasonably consistent in reference to the distance from the center of the city. The r value in the second (dispersed) type cities (mean = 0.58) was generally higher than that in the first (concentrated) type cities (mean = 0.48). The urban expansion in the second-type cities conforms more to the patterns of concentric zonation.

Conclusions

The urban growth effects on vegetative greenness as measured from Landsat TM data have been examined in this study. The findings indicate that there was a remarkable expansion in urban land cover in the Zhujiang Delta, China, between 1989 and 1997. Urban land development was uneven among administrative units. The spatial process of urban expansion showed an intimate relationship with the distances from major roads and urban centers. Urban land development tends to bring down vegetative greenness. The spatial patterns of vegetative greenness decrease are correlated with the pattern of urban expansion. This is particularly true when all these patterns are referenced to major roads or to urban centers.

The digital image classification with Landsat TM data coupled with GIS has demonstrated its sufficient capability to provide comprehensive information on the direction, nature, rate, and location of land use and land cover changes as a result of rapid industrialization and urbanization. Useful information can be derived by using some fundamental GIS functions such as buffer, overlay, and database query. In association with spatial analytical techniques, including the computation of an entropy index, GIS-based analysis proves to be sufficiently powerful in confirming the patterns and processes of urban expansion. Biophysical measurements such as vegetative greenness can be extracted from Landsat TM images, and be related to land use and land cover data to examine the environmental impacts of urban growth.

One basic objective of this study is to develop methodologies for the integration of remote sensing, GIS, and spatial analysis techniques for evaluation of urban growth and its impact on the environment. The technology of remote sensing collects multi-spectral, multi-spatial, and multi-temporal data, and turns them into information valuable for environmental studies. GIS technology provides a flexible environment for inputting, analyzing, and displaying digital data from various sources, and can incorporate socioeconomic data necessary for environmental problem solving. However, to examine complex environmental problems, GIS needs to be further integrated with spatial analysis techniques. This study has demonstrated that the integration among the three elements can reinforce one another, and is imperative in assessing the environmental impacts of land use and land cover change.

Acknowledgments

The funding support of the National Geographic Society, which made our fieldwork possible, is gratefully acknowledged. The authors also wish to thank anonymous reviewers for their constructive comments and suggestions, and Craig W. Remington for making the study area map. Qihao Weng acknowledges the financial support of Research Advisory Committee at the University of Alabama.

References

Anderson, J. R., Hardy, E. E., Roach, J. T., and R.E. Witmer, 1976, *A Land Use and Land Cover Classification Systems for Use with Remote Sensing Data*, USGS Professional Paper 964.

ASPRS, 1994, *Remote Sensing and Geographic Information Systems: An Integration of Technologies for Resource Management*, ASPRS, Bethesda, MD.

Atkinson, P. M, and N. J. Tate, 1999, Techniques for the analysis of spatial data. *Advances in Remote Sensing and GIS Analysis* (P. M. Atkinson and N. J. Tate, editors), John Wiley & Sons, New York, pp. 1-5.

Che, N., and J. C. Price, 1992, Survey of radiometric calibration results and methods for visible and near infrared channels of NOAA-7, -9 and -11 AVHRRs. *Remote Sensing of Environment*, 50: 1-7.

Ditu Chubanshe, 1977, *Provincial Atlas of the People's Republic of China*, People's Press, Beijing.

Dymond, J. R., Page, M. J., and L. J. Brown, 1996, Large area vegetation mapping in the Gisborne district, New Zealand, from Landsat TM, *International Journal of Remote Sensing*, 17 (2): 263-275.

Ehlers, M., Jadkowski, M. A., Howard, R. R., and D. E. Brostuen, 1990, Application of SPOT data for regional growth analysis and local planning, *Photogrammetric Engineering and Remote Sensing, 56* (2): 175-180.

Ekstrand, S., 1996, Landsat TM-based forest damage assessment: correction for topographic effects. *Photogrammetric Engineering & Remote Sensing*, 62(1): 151-161.

Foody, G. M., and R. A. Hill, 1996, Classification of tropical forest classes from Landsat TM data, *International Journal of Remote Sensing*, 17(12): 2353-2367.

Gillies, R. R., Carlson, T. N., Cui, J., Kustas, W. P., and K. S. Humes, 1997, A verification of the 'triangle' method for obtaining surface soil water content and energy fluxes from remote measurements of the Normalized Difference Vegetation index (NDVI) and surface radiant temperature, *International Journal of Remote Sensing*, 18(15): 3145-3166.

Gong, Z., and Z. Chen, 1964, The soils of the Zhujiang River Delta. *Journal of Soils*, 36: 69-124. (In Chinese)

Harris, P. M., and S. J. Ventura, 1995, The integration of geographic data with remotely sensed imagery to improve classification in an urban area, *Photogrammetric Engineering and Remote Sensing*, 61: 993-998.

Hinton, J. C., 1996, GIS and remote sensing integration for environmental applications, *International Journal of Geographic Information Systems*, 10(7): 877-890.

Jakubauskas, M.E., and K.P. Price, 1994, Landsat thematic mapper characterization of coniferous forest succession, *Proceedings of ASPRS/ACSM 1994*, Reno, Nevada, pp. 256-267.

Jensen, J. R., 1996, *Introductory Digital Image Processing: A Remote Sensing Perspective* (Second Edition), Prentice Hall, Upper Saddle River, NJ.

Jensen, J. R., Rutchey, K., Koch, M. and S. Narumalani. 1995. Inland wetland change detection in the Everglades water conservation area 2A using a time series of normalized remotely sensed data. *Photogrammetric Engineering & Remote Sensing*, 61(2): 199-209.

Knick, S. T., Rotenberry, J.T., and T. J. Zarriello, 1997, Supervised classification of Landsat Thematic Mapper imagery in a semi-arid rangeland by nonparametric discriminant analysis, *Photogrammetric Engineering & Remote Sensing*, 63(1): 79-86.

Li, Y., Mausel, P., Wu, Y., Moran, E., E. Brondizio, 1994, Discrimination between advanced secondary succession and mature moist forest near Altamira, Brazil, using Landsat TM data. *Proceedings of ASPRS/ACSM 1994*, Reno, Nevada, pp. 350-364.

Lo, C. P., 1989, Recent spatial restructuring in Zhujiang Delta, South China: A study of socialist regional development strategy, *Annals of the Association of the American Geographers*, 79(2): 293-308.

Lo, C. P., and L. J. Watson, 1994, Okefenokee Swamp vegetation mapping with Landsat thematic mapper data: an evaluation, *Proceedings of ASPRS/ACSM 1994*, Reno, Nevada, pp. 365-374.

Mesev, V., 1997, Remote sensing of urban systems: hierarchical integration with GIS, *Computer, Environment, and Urban Systems*, 21 (3-4): 175-187.

Nissan, E., and G. Carter, 1994, Measuring interstate and interregional income inequality in the United States, *Economic Development Quarterly*, 8(4): 364-372.

Price, J. C., 1987, Calibration of satellite radiometers and the comparison of vegetation indices, *Remote Sensing of Environment*, 21: 15-27.

Sader, S. A., Stone, T. A., and A. T. 1990, Remote sensing of tropical forests: an overview of research and applications using non-photographic sensors, *Photogrammetric Engineering and Remote Sensing*, 55(10): 1343-1351.

Sader, S. A., 1994, Spatial analysis of tropical forest change in northern Guatemala. *Proceedings of ASPRS/ ACSM 1994*, Reno, Nevada, pp. 551-557.

Star, J. L. (ed.), 1991, *The Integration of Remote Sensing and Geographic Information Systems*, American Society for Photogrammetry and Remote Sensing, Bethesda, Maryland.

Star, J. L., Estes, J. E., and K. C. McGwire, 1997, *Integration of Geographic Information Systems and Remote Sensing*, Cambridge University Press, Cambridge.

Statistical Bureau of Guangdong, 1998, *Statistical Yearbook of Guangdong 1997*, China Statistics Press, Beijing.

Steininger, M. K., 1996, Tropical secondary forest regrowth in the Amazon: age, area and change estimation with Thematic Mapper data, *International Journal of Remote Sensing*, 17(1): 9-27.

Theil, H., 1967, *Economics and Information Theory*, North-Holland, Amsterdam.

Thenkabail, P. S., Ward, A. D., Lyon, J. G., and C. J. Merry, 1994, Thematic Mapper vegetation indices for determining soybean and corn growth parameters, *Photogrammetric Engineering & Remote Sensing*, 60(4): 437-442.

Treitz, P. M., Howard, P. J., and P. Gong, 1992, Application of satellite and GIS technologies for land-cover and land-use mapping at the rural-urban fringe: A case study, *Photogrammetric Engineering and Remote Sensing*, 58(4): 439-448.

Weng, Q., 1998, Local impacts of the post-Mao development strategy: the case of the Zhujiang Delta, southern China, *International Journal of Urban and Regional Studies*, 22(3): 425-442.

Weng, Q., 2001, A remote sensing-GIS evaluation of urban expansion and its impact on surface temperature in the Zhujiang Delta, China, *International Journal of Remote Sensing*, 22(10): 1999-2014.

Yeh, A. G. O., and X. Li, 1996, Urban growth management in the Pearl River delta - an integrated remote sensing and GIS approach, *The ITC Journal*, 1: 77-85.

Yeh, A. G. O., and X. Li, 1997, An integrated remote sensing-GIS approach in the monitoring and evaluation of rapid urban growth for sustainable development in the Pearl River Delta, China, *International Planning Studies*, 2(2): 193-210.

Yeh, A. G. O., and X. Li, 1999, Economic development and agricultural land loss in the Pearl River Delta, China, *Habitat International*, 23(3): 373-390.